Biochimica et Biophysica Acta 1853 (2015) 3182–3191

Contents lists available at ScienceDirect

Biochimica et Biophysica Acta

journal homepage: www.elsevier.com/locate/bbamcr

Intracellular magnesium level determines cell viability in the MPP^+ model of Parkinson's disease

Yutaka Shindo [a], Ryu Yamanaka [a], Koji Suzuki [b], Kohji Hotta [a], Kotaro Oka [a,*]

[a] Department of Bioscience and Informatics, Faculty of Science and Technology, Keio University, 3-14-1 Hiyoshi, Kohoku-ku, Yokohama, Kanagawa 223-8522, Japan
[b] Department of Applied Chemistry, Faculty of Science and Technology, Keio University, 3-14-1 Hiyoshi, Kohoku-ku, Yokohama, Kanagawa 223-8522, Japan

ARTICLE INFO

Article history:
Received 20 April 2015
Received in revised form 24 July 2015
Accepted 22 August 2015
Available online 28 August 2015

Keywords:
Magnesium
Parkinson's disease
Reactive oxygen species
ATP
Neuroprotection
Mitochondria

ABSTRACT

Parkinson's disease (PD) is a neurodegenerative disorder resulting from mitochondrial dysfunction in dopaminergic neurons. Mitochondria are believed to be responsible for cellular Mg^{2+} homeostasis. Mg^{2+} is indispensable for maintaining ordinal cellular functions, hence perturbation of the cellular Mg^{2+} homeostasis may be responsible for the disorders of physiological functions and diseases including PD. However, the changes in intracellular Mg^{2+} concentration ($[Mg^{2+}]_i$) and the role of Mg^{2+} in PD have still been obscure. In this study, we investigated $[Mg^{2+}]_i$ and its effect on neurodegeneration in the 1-methyl-4-phenylpyridinium (MPP^+) model of PD in differentiated PC12 cells. Application of MPP^+ induced an increase in $[Mg^{2+}]_i$ immediately via two different pathways: Mg^{2+} release from mitochondria and Mg^{2+} influx across cell membrane, and the increased $[Mg^{2+}]_i$ sustained for more than 16 h after MPP^+ application. Suppression of Mg^{2+} influx decreased the viability of the cells exposed to MPP^+. The cell viability correlated highly with $[Mg^{2+}]_i$. In the PC12 cells with suppressed Mg^{2+} influx, ATP concentration decreased and the amount of reactive oxygen species (ROS) increased after an 8 h exposure to MPP^+. Our results indicate that the increase in $[Mg^{2+}]_i$ inhibited cellular ROS generation and maintained ATP production, which resulted in the protection from MPP^+ toxicity.

1. Introduction

Parkinson's disease (PD) is a neurodegenerative disorder that is caused by degradation of dopaminergic neurons in substantia nigra [1]. Previous studies have demonstrated that the neuronal disorder is accompanied by mitochondrial dysfunction [2,3]. In the dopaminergic neurons in PD patients, mitochondrial morphological changes and down-regulation of their function have been reported [4,5]. Moreover, mutations in genes owing to mitochondrial quality control relate to familial PD [6,7], indicating that mitochondrial dysfunction was crucially involved in PD. Inhibitors of complex I in the mitochondrial electron transfer chain, such as 1-methyl-4-phenylpyridinium (MPP^+) and rotenone, induce PD-like degeneration in dopaminergic cells. Investigations of cell death induced by these reagents are expected to clarify the underlying mechanism of neurodegeneration in PD [1]. Down-regulation of mitochondrial functions results in the depletion of cellular ATP, generation of reactive oxygen species (ROS) [8] and finally the release of apoptosis inducers to the cytoplasm [9,10]. Therefore, it can be concluded that mitochondria play a pivotal role in PD.

In previous studies conducted by our group, it was demonstrated that mitochondria play an important role in cellular Mg^{2+} homeostasis [11–14]. Mg^{2+} is an essential cation for a number of physiological processes including mitochondrial functions [15,16]. The Mg^{2+} concentration in mitochondria modulates mitochondrial ATP synthesis [17,18]. Mg^{2+} around mitochondria suppresses Ca^{2+}-induced ROS generation and the formation of mitochondrial permeability transition pore [19]. These reports indicate that Mg^{2+} transport across the cellular and mitochondrial membrane is involved in the regulation of cellular energy metabolism and apoptosis. Recent studies have demonstrated the importance of Mg^{2+} in cellular functions further: second messenger role in T-cells [20], regulation of neuronal development [21], and modulation of electric synapses [22]. Due to the importance of this ion, deficiency of Mg^{2+} has been linked to the disorder of physiological functions and diseases including PD [23,24]. However, whether the intracellular Mg^{2+} concentration ($[Mg^{2+}]_i$) changes in neuronal disorders and whether it plays pivotal roles in the process of disease have still been obscure.

Low Mg^{2+} concentrations in the brain tissues of PD patients have previously been reported [23]. We also demonstrated that MPP^+, which induces PD-like dopaminergic cell death, induced acute Mg^{2+} release from mitochondria in PC12 cells [25]. These studies suggest that the perturbation of Mg^{2+} in the cells and in the mitochondria would be involved in the process of neurodegeneration in PD. Moreover, it has been reported that Mg^{2+} supplementation in a culture medium protects cells from neurodegeneration in cellular model of PD [26], suggesting that Mg^{2+} may have important role in neuroprotection. In this

* Corresponding author.
E-mail address: oka@bio.keio.ac.jp (K. Oka).

http://dx.doi.org/10.1016/j.bbamcr.2015.08.013
0167-4889/

study, we investigated the MPP^+-induced chronic changes in $[Mg^{2+}]_i$ and its mechanisms. We also estimated the contribution of intracellular Mg^{2+} to cell viability in the MPP^+ model of PD in PC12 cells.

2. Materials and methods

2.1. Cell culture

PC12 cells were obtained from the Riken Tsukuba Institute, and cultured in a Dulbecco's modified Eagle's medium (DMEM) containing 10% horse serum, 5% fetal bovine serum (FBS), 50 U/mL penicillin and 50 μg/mL streptomycin at 37 °C in the CO_2 incubator. For fluorescence measurements, the cells were cultured on poly-D-lysine (PDL)-coated glass bottom dishes. For experimental use, cells were differentiated by culturing in a serum-free medium with 50 ng/mL nerve growth factor (NGF) for 5 days.

2.2. Fluorescence imaging

To measure the changes in $[Mg^{2+}]_i$ and intracellular Ca^{2+} concentration ($[Ca^{2+}]_i$), mag-fura-2-AM and fura-2-AM (Invitrogen, Carlsbad, CA, USA) were used, respectively. Mag-fura-2-AM or fura-2-AM was applied to the culture medium at 2 μM, and the cells were incubated at 37 °C for 30 min. The cells were then washed twice with an experimental medium containing (in mM): NaCl, 125; KCl, 5; $CaCl_2$, 2; $MgSO_4$, 1.2; KH_2PO_4, 1.2; D-glucose, 6; HEPES, 25 (pH adjusted to 7.4 with NaOH) and further incubated in the experimental medium at 37 °C for 15 min to allow for complete hydrolysis of the acetoxymethyl (AM) ester form. For the experiments performed in Mg^{2+}-free or Ca^{2+}-free condition, the experimental medium was replaced to the medium without $MgSO_4$ (nominally Mg^{2+}-free experimental medium) or that without $CaCl_2$ (nominally Ca^{2+}-free experimental medium) at the washing procedure, and cells were incubated at 37 °C for 15 min to allow complete hydrolysis of the AM ester form of fluorescent dyes in each medium. Osmolarity of normal, nominally Mg^{2+}-free and nominally Ca^{2+}-free experimental medium were 296, 294 and 291 mOsmol/kg, respectively. The osmolarity was measured with a freezing point osmometer, OSMOMAT 3000D (Gonotec, Berlin, Germany). In some experiments, mag-fura-2-AM was used at 10 μM to chelate intracellular Mg^{2+}.

Fluorescence of mag-fura-2 and fura-2 were measured on a fluorescence microscope ECLIPSE TE300 (Nikon, Tokyo, Japan) equipped with a 20× objective lens (S Fluor, Nikon). A 150 W Xe lamp was used as the source of excitation, and a light of a suitable wavelength was selected with the monochrometer unit. Mag-fura-2 and fura-2 were excited at 340 nm (Mg^{2+} or Ca^{2+} bound) and 380 nm (Mg^{2+} or Ca^{2+} unbound), alternatively. The fluorescence was detected with a CCD camera (HiSCA, Hamamatsu photonics, Shizuoka, Japan) through a 400 nm dichroic mirror and a 535/55 nm emission filter. Analysis was conducted with Aquacosmos software (Hamamatsu photonics). Fluorescence intensities were calculated as mean intensities in the region of interest (ROI) containing the entire cell body.

2.3. Calibration of $[Mg^{2+}]_i$ and $[Ca^{2+}]_i$

$[Mg^{2+}]_i$ and $[Ca^{2+}]_i$ were estimated from the fluorescence ratio of mag-fura-2 and fura-2 respectively, following a previous study [27]. To estimate R_{max} and R_{min} for mag-fura-2, PC12 cells were incubated in a high-Mg^{2+} medium containing (in mM): NaCl, 125; KCl, 5; $MgSO_4$, 100; KH_2PO_4, 1.2; D-glucose, 6; HEPES, 25 (pH adjusted to 7.4 with NaOH) or in Mg^{2+}-chelated medium added 50 mM EDTA to the experimental medium for 10 min with 0.00125% digitonin. Digitonin was washed out and cells were further incubated in the high-Mg^{2+} medium or Mg^{2+}-chelated medium for 30 min. Then, the cells were stained with mag-fura-2, and fluorescence was measured in these media, respectively. To estimate R_{max} and R_{min} for fura-2, fura-2 loaded PC12 cells were incubated in the experimental medium or absolutely Ca^{2+}-free medium containing (in mM): NaCl, 125; KCl, 5; $MgSO_4$, 1.2; KH_2PO_4, 1.2; EGTA, 1; D-glucose, 6; HEPES, 25 (pH adjusted to 7.4 with NaOH) for 15 min with 5 μM ionocycin. Then, the fluorescence was measured.

2.4. Measurement of intracellular total divalent cation concentration

Total amounts of intracellular Ca^{2+} and Mg^{2+} were measured with inductively coupled plasma atomic emission spectroscopy (ICP-AES). Control and MPP^+ treated cells were washed twice using PBS, harvested in ice-cold PBS and centrifuged at 4 °C, 800 ×g for 3 min. The supernatant was discarded, the cells were resuspended in 1 mL ice-cold PBS and sonicated. 200 μL of cell lysate was used to measure protein concentration in the sample. Mg^{2+} and Ca^{2+} concentrations in the remaining 800 μL were measured with ICP-AES at Shimadzu Techno-Research (Kyoto, Japan). Protein concentration in each sample was measured using a protein assay with coomassie brilliant blue (CBB) (Nakaraitesqu, Osaka, Japan). Absorbance at 570 nm was measured with a microplate reader (Fluoroskan Ascent FL, Thermo Fisher Scientific, Waltham, MA, USA). Mg^{2+} and Ca^{2+} concentrations measured with ICP-AES were normalized to the protein concentration in each sample.

2.5. Measurement of cell viability

Cell viability was measured using the MTT assay. After exposure to MPP^+, the culture medium was replaced with the medium containing 0.5 mg/mL of MTT, and cells were incubated for 2 h at 37 °C. The culture medium was removed and 100 μL of dimethyl sulfoxide was added in each well to dissolve the precipitation, and the absorbance at 570 nm was measured using a microplate reader. Cell viability was calculated as a ratio of the control culture value.

2.6. Stable expression of SLC41A2 in PC12 cells

Total RNA was isolated from PC12 cells and purified using the RNeasy mini kit (QIAGEN, Tokyo, Japan). The total RNA was treated with TURBO DNase (Ambion, CA, USA), and single-stranded cDNA was generated by reverse transcription using SuperScript VILO (Invitrogen). DNA coding SLC41A2 was amplified with PCR and inserted in the pEGFP-C1 vector (Takara, Siga, Japan) at the BglII and the ApaI restriction enzyme sites. The vector was transfected to PC12 cells with Lipofectamine LTX. Two days after transfection, the cells were cultured and screened in the culture medium containing 500 ng/mL of genetisin (Invitrogen) for 2 weeks. The remaining cells, most of which likely possess the transfected gene, were suspended, diluted to 2.5 cells/mL in the culture medium containing genetisin and plated in a 96 well plate (200 μL for each well). The wells containing only one cell were selected, and the expression of EGFP was confirmed. The cells that emit EGFP fluorescence and can proliferate in genetisin containing the medium were the ones stably expressing the transfected gene.

2.7. Real-time PCR

Total RNA from PC12 cells were isolated and purified by using the RNeasy mini kit. The total RNA was treated with Terbo DNase, and single-stranded cDNA was generated by reverse transcription by using SuperScript VILO. Real-time PCR was carried out with SYBR GreenER™ (Invitrogen). Primers used were as follows: for SLC41A2 (forward primer, 5′- ATTACCTCAGCCATTCCATACTCC; reverse primer, 5′- AGCCAACGATAA CTCCAACCA) and for hydroxymethiylbilane synthase (Hmbs), (forward primer, 5′- TCTAGATGGCTCAGATAGCATGCA; reverse primer, 5′- TGGA CCATCTTCTTGCTGAACA). Hmbs was used as a housekeeping gene. Real-time PCR was performed by using Rotor-Gene (QIAGEN) for 40 cycles. Data was quantified with the comparative Ct quantification method by plotting cycle number at threshold. Expression levels of SLC41A2 were

normalized to that of HMBS. Relative expression levels to average in control PC12 cells were compared.

2.8. Measurement of intracellular ATP concentration

To measure intracellular ATP concentration, a genetically encoded ATP sensor, ATeam, was expressed in PC12 cells [28]. Four days after NGF supplementation, the plasmid coding ATeam was transfected to the PC12 cells by using Lipofectamine LTX (Invitrogen). The next day, cells were exposed to MPP^+ and the fluorescence signals of ATeam were observed.

The fluorescence of ATeam was measured using a confocal laser scanning microscope system (FluoView FV1000, Olympus, Tokyo, Japan) mounted on an inverted microscope (IX81, Olympus) with a 40× oil-immersion objective lens. ATeam was excited at 440 nm from the laser diode, and the fluorescence signals were separated using a 510 nm dichroic mirror and observed at 460–500 nm for cyan fluorescent protein (CFP) and 515–615 nm for yellow fluorescent protein (YFP). Fluorescence images were acquired with photomultipliers and analyzed with the FluoView software package (Olympus). Fluorescence intensities were calculated as the mean intensity over a defined ROI containing the entire cell body of each cell. The intracellular ATP concentration corresponds to the fluorescence ratio (YFP/CFP).

2.9. Measurement of intracellular ROS

Intracellular ROS was measured using a total ROS detection kit (Enzo Life Sciences, New York, USA). Differentiated PC12 cells were exposed to 0 or 3 mM MPP^+ for 8 h. The MPP^+ containing a culture medium was replaced with a culture medium containing 500 nM of an oxidative stress detection reagent. The cells were incubated at 37 °C for 30 min and washed twice with a wash buffer. The dish was then filled with a fresh experimental medium. Fluorescence was measured with a fluorescence microscope, ECLIPSE TE300 as described above. The probe was excited at 488 nm and the fluorescence was detected with a CCD camera through a 505 nm dichroic mirror and a 535/55 nm emission filter.

2.10. Statistical analysis

Significant differences were determined using the Student's *t*-test for the comparison of two sets of data and using Dunnett's test for multiple comparisons. The *P* values of less than 0.05 were considered to be significantly different.

3. Results

3.1. MPP^+ induces dosage- and time-dependent cell death in differentiated PC12 cells

The dosage- and time-dependent change in viability of PC12 cells to MPP^+ toxicity were estimated. We found that exposure to 3 mM of MPP^+ for 24 h induced about 50% cell death (Fig. S1A). Relationship between the concentration of MPP^+ and the cell viability was in agreement with the previously reported study on MPP^+ toxicity using differentiated PC12 cells [9]. In the medium containing 3 mM of MPP^+, the cell viability did not change for 6 h, and it decreased to 90% in 8 h and to 70% in 16 h (Fig. S1B). Based on these results, MPP^+ at a concentration of 3 mM was used, and the effects of MPP^+ at the onset of the cell death (8 h) and/or at the further progressed stage (16 h) were estimated.

3.2. MPP^+ immediately alters intracellular divalent cation concentration

To estimate the effects of MPP^+ on intracellular divalent cation concentration, changes in $[Mg^{2+}]_i$ and $[Ca^{2+}]_i$ were measured using mag-fura-2 and fura-2, respectively. These probes are useful tools to compare the $[Mg^{2+}]_i$ and $[Ca^{2+}]_i$ quantitatively in the cells under various conditions, because they are ratiometric probes. Although mag-fura-2 has been used as a fluorescent Mg^{2+} probe, it is sometimes used as a low affinity Ca^{2+} indicator [29] because it has a low K_d value for Ca^{2+} [30]. Therefore, we must confirm that the fluorescent signal from mag-fura-2 results not from Ca^{2+} but from Mg^{2+}.

At first, changes in $[Mg^{2+}]_i$ and $[Ca^{2+}]_i$ immediately after MPP^+ application were observed. $[Mg^{2+}]_i$ in differentiated PC12 cells was calibrated using mag-fura-2 ratio. It was about 0.5 mM in the steady state. MPP^+ induced an increase in $[Mg^{2+}]_i$ to about 0.65 mM immediately after its application, and $[Mg^{2+}]_i$ maintained the increased level for more than 10 min (Fig. 1A and B). $[Ca^{2+}]_i$ in the steady state was estimated to be about 80 nM. $[Ca^{2+}]_i$ also increased to about 130 nM in 2 min in response to MPP^+ application, and then decreased to basal concentration gradually (Fig. 1C). In a nominally Ca^{2+}-free experimental medium, $[Ca^{2+}]_i$ in steady state was low (about 20 nM), and an increase in $[Ca^{2+}]_i$ in response to MPP^+ was abolished (Fig. 1C and D). The increase in the mag-fura-2 signal in response to MPP^+ was not changed in a nominally Ca^{2+}-free experimental medium (Fig. 1B). Therefore, we concluded that the change in the mag-fura-2 signal indicated the change in $[Mg^{2+}]_i$ without interference from the Ca^{2+} signal.

Our previous study demonstrated that MPP^+ elicits a decrease in Mg^{2+} concentration in mitochondria in PC12 cells by monitoring the change in the Mg^{2+} concentration inside the mitochondria [25]. It is likely that the Mg^{2+} was released from the mitochondria to the cytoplasm. To further study the Mg^{2+} release, MPP^+ was applied to the cells pretreated with carbonyl cyanide p-(trifluoromethoxy) phenylhydrazone (FCCP). FCCP is an uncoupler for the mitochondrial inner membrane, and the collapse of their membrane potential induces Mg^{2+} release from mitochondria [14]. Therefore, pre-treatment with FCCP would abolish MPP^+-induced Mg^{2+} release from mitochondria. FCCP was added to an experimental medium 10 min prior to MPP^+ application. FCCP induced about 0.4 mM increase in $[Mg^{2+}]_i$ (from 0.5 to 0.9 mM, Fig. S2). Whereas $[Mg^{2+}]_i$ also increased in response to following MPP^+ application, the increased concentration (about 0.1 mM) was a significantly smaller value than control (Fig. 1B). It indicates that mitochondria partly contribute to the increase in $[Mg^{2+}]_i$, and there might be other mechanisms to induce the increase in $[Mg^{2+}]_i$ in response to MPP^+ application.

To evaluate the contribution of Mg^{2+} influx, $[Mg^{2+}]_i$ was measured in a nominally Mg^{2+}-free experimental medium. Whereas $[Mg^{2+}]_i$ in steady state was not affected in a nominally Mg^{2+}-free experimental medium, the increase in $[Mg^{2+}]_i$ was significantly attenuated. Moreover, it was completely suppressed in the cells pre-treated with FCCP in the nominally Mg^{2+}-free experimental medium (Fig. 1C and D). These results indicate that an MPP^+-induced increase in $[Mg^{2+}]_i$ was composed of Mg^{2+} mobilization via two different pathways: Mg^{2+} influx and Mg^{2+} release from mitochondria. On the other hand, the increase in $[Ca^{2+}]_i$ was mostly abolished in a nominally Ca^{2+}-free experimental medium, and pretreatment with FCCP had no effect on it in the nominally Ca^{2+}-free experimental medium (Fig. 1C and D). These results indicate that the increase in $[Ca^{2+}]_i$ mainly results from Ca^{2+} influx.

TRPM7, which is a cation channel expressing on cell membrane, plays an important role in cellular Mg^{2+} homeostasis [31]. We examined the contribution of these channels to the $[Mg^{2+}]_i$ increase. The increases in $[Mg^{2+}]_i$ and $[Ca^{2+}]_i$ in response to MPP^+ were significantly attenuated in the presence of 50 μM of 2-aminoethoxydiphenyl borate (2-APB) (Fig. 1B and D), which is an inhibitor of Ca^{2+} permeable channels including TRPM7 [32,33]. It suggests that MPP^+ or a downstream intracellular signal activated Mg^{2+} influx and Ca^{2+} influx via TRPM7. Moreover, the Mg^{2+} influx was partly suppressed by 40 μM of imipramine (Fig. 1B). Imipramine was used at the concentration that has no toxicity to differentiated PC12 cells for 16 h. Although imipramine is known as an inhibitor of Na^+/Mg^{2+} exchanger working as Mg^{2+} extrusion mechanism, it also inhibits Mg^{2+} influx via TRPM-like channel [34] and via reversible type Na^+/Mg^{2+} exchanger [35] across a cell

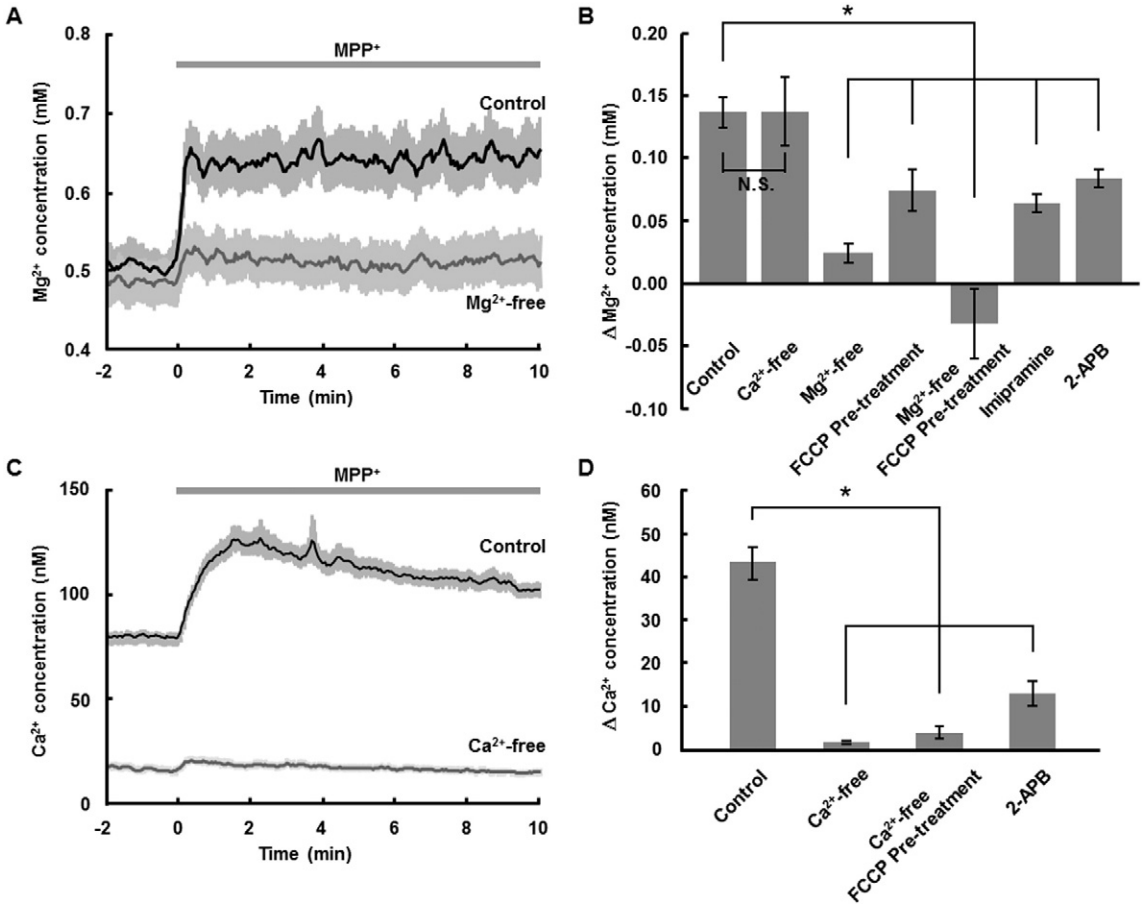

Fig. 1. Changes in $[Mg^{2+}]_i$ immediately after MPP^+ application. (A) Averaged time-courses of $[Mg^{2+}]_i$ in response to MPP^+ (3 mM) in normal experimental medium (control; black line, n = 207 cells from 16 experiments) and nominally Mg^{2+}-free experimental medium (gray line, n = 105 cells from 8 experiments). (B) Comparison of the changes in $[Mg^{2+}]_i$ in response to MPP^+ under various conditions (Control (normal experimental medium), n = 207 cells from 16 experiments; Ca^{2+}-free (nominally Ca^{2+}-free experimental medium), n = 77 cells from 7 experiments; Mg^{2+}-free (nominally Mg^{2+}-free medium), n = 105 cells from 8 experiments; FCCP (5 μM) pre-treatment, n = 110 cells from 8 experiments; Mg^{2+}-free FCCP pre-treatment, n = 60 cells from 5 experiments; Imipramine (40 μM), n = 108 cells from 8 experiments; 2-APB (50 μM), n = 156 from 11 experiments). The change in $[Mg^{2+}]_i$ was calculated as the difference between averaged concentration from −1 to 0 min and that from 4 to 5 min in time-course of each cell. (C) Averaged time-courses of $[Ca^{2+}]_i$ in response to MPP^+ in normal experimental medium (control; black line, n = 186 cells from 9 experiments) and nominally Ca^{2+}-free experimental medium (gray line, n = 169 cells from 9 experiments). (D) Comparison of the changes in $[Ca^{2+}]_i$ in response to MPP^+ under various conditions (Control (normal experimental medium), n = 186 cells from 9 experiments; Ca^{2+}-free (nominally Ca^{2+}-free experimental medium), n = 169 cells from 9 experiments; Ca^{2+}-free FCCP Pre-treatment, n = 50 cells from 3 experiments; 2-APB, n = 60 cells from 4 experiments). Time-courses and bar graphs are represented as mean ± SEM. * indicates $P < 0.05$ in Dunnett's test.

membrane. This result also demonstrates that MPP^+ induces Mg^{2+} influx across the cell membrane.

3.3. Mg^{2+} influx causes a sustained increase in intracellular Mg^{2+}

MPP^+ induced an increase in $[Mg^{2+}]_i$ and $[Ca^{2+}]_i$ immediately after its application, and $[Mg^{2+}]_i$ remained at the increased concentration for at least 10 min while $[Ca^{2+}]_i$ gradually decreased in 10 min. To determine the changes in divalent cation concentrations depending on the progress of the cell death induced by MPP^+, $[Mg^{2+}]_i$ and $[Ca^{2+}]_i$ in the cells exposed to MPP^+ for 8 and 16 h were measured and compared with those in the cells not exposed to MPP^+ (control). The $[Mg^{2+}]_i$ in the cells exposed to MPP^+ for 8 and 16 h remained higher (about 0.7 mM) than that in non-exposed cells (Fig. 2A). On the other hand, $[Ca^{2+}]_i$ in the cells exposed to MPP^+ for 8 h showed almost the same levels to non-exposed cells (8 h and control in Fig. 2B). It indicates that MPP^+ induced a transient increase in $[Ca^{2+}]_i$ immediately after its application, and then $[Ca^{2+}]_i$ returned to the basal level and remained in it for at least 8 h. $[Ca^{2+}]_i$ increased again after a 16 h exposure to MPP^+; it probably resulted from the increase in $[Ca^{2+}]_i$ as a cell death signal [36]. These results indicate that MPP^+ induced-$[Ca^{2+}]_i$ increase has two phases. The time-course in $[Ca^{2+}]_i$ was different from that in $[Mg^{2+}]_i$. It also makes sure that the changes in mag-fura-2 ratio were the result of changes in $[Mg^{2+}]_i$ not the changes in $[Ca^{2+}]_i$.

Cellular total Mg^{2+} and Ca^{2+} contents were measured to determine that the increase in $[Mg^{2+}]_i$ results from Mg^{2+} influx. More than 90% of cellular Mg^{2+} is not free and is bound to intracellular biological molecules, hence $[Mg^{2+}]_i$ might be altered without ion transport across the cell membrane. If the increase in $[Mg^{2+}]_i$ originated from the extracellular medium, total cellular Mg^{2+} content would increase. Therefore, the total cellular Mg^{2+} and Ca^{2+} contents were measured with ICP-AES. Total cellular Mg^{2+} content significantly increased at 16 h (Fig. 2C), whereas total Ca^{2+} content did not alter in 16 h (Fig. 2D). These results indicate that MPP^+ induced a continuous Mg^{2+} influx. This caused a sustained increase in $[Mg^{2+}]_i$ and an increase in cellular total Mg^{2+} content after 16 h.

3.4. Intracellular Mg^{2+} level determines cell viability

The Mg^{2+} influx contributed to the increase in $[Mg^{2+}]_i$, hence its inhibition would alter the $[Mg^{2+}]_i$ after 16 h. As shown in Fig. 1B, the Mg^{2+} influx induced by MPP^+ was suppressed in nominally Mg^{2+}-free medium and also in an imipramine containing medium. 16 h after exposure to MPP^+, MPP^+-induced increase in $[Mg^{2+}]_i$ was also suppressed under those conditions, whereas it was potentiated under high Mg^{2+}

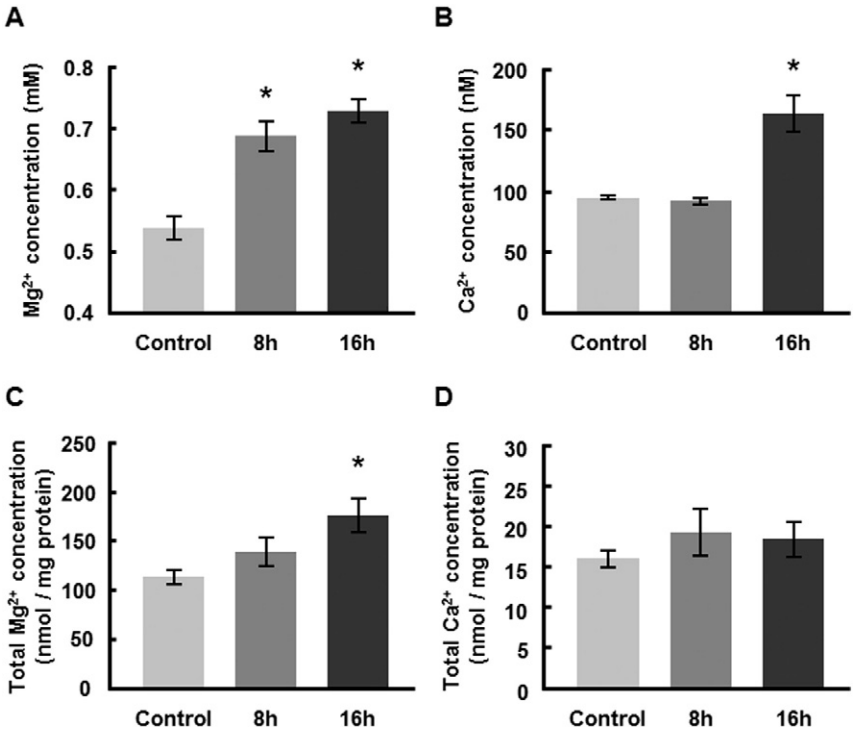

Fig. 2. Comparison of intracellular Mg^{2+} and Ca^{2+} concentrations. (A) $[Mg^{2+}]_i$ in the cells not exposed to MPP^+ (Control, n = 341 cells from 7 experiments) and in the cells exposed to 3 mM of MPP^+ for 8 h (n = 198 cells from 4 experiments) and 16 h (n = 392 cells from 5 experiments) were compared. $[Mg^{2+}]_i$ was calculated from mag-fura-2 ratio. (B) $[Ca^{2+}]_i$ in the cells not exposed to MPP^+ (control, n = 1077 cells from 10 experiments) and in the cells exposed to 3 mM of MPP^+ for 8 h (n = 687 cells from 7 experiments) and 16 h (n = 649 cells from 7 experiments) were compared. $[Ca^{2+}]_i$ was calculated from fura-2 ratio. (C) Cellular total Mg^{2+} concentration in the cells not exposed to MPP^+ (control) and in the cells exposed to 3 mM of MPP^+ for 8 and 16 h were compared (n = 3 samples for each condition). (D) Intracellular total Ca^{2+} concentration in the cells not exposed to MPP^+ (control) and in the cells exposed to 3 mM of MPP^+ for 8 and 16 h were compared (n = 3 samples for each condition). Data are represented as mean ± SEM. * indicates $P < 0.05$ in Dunnett's test.

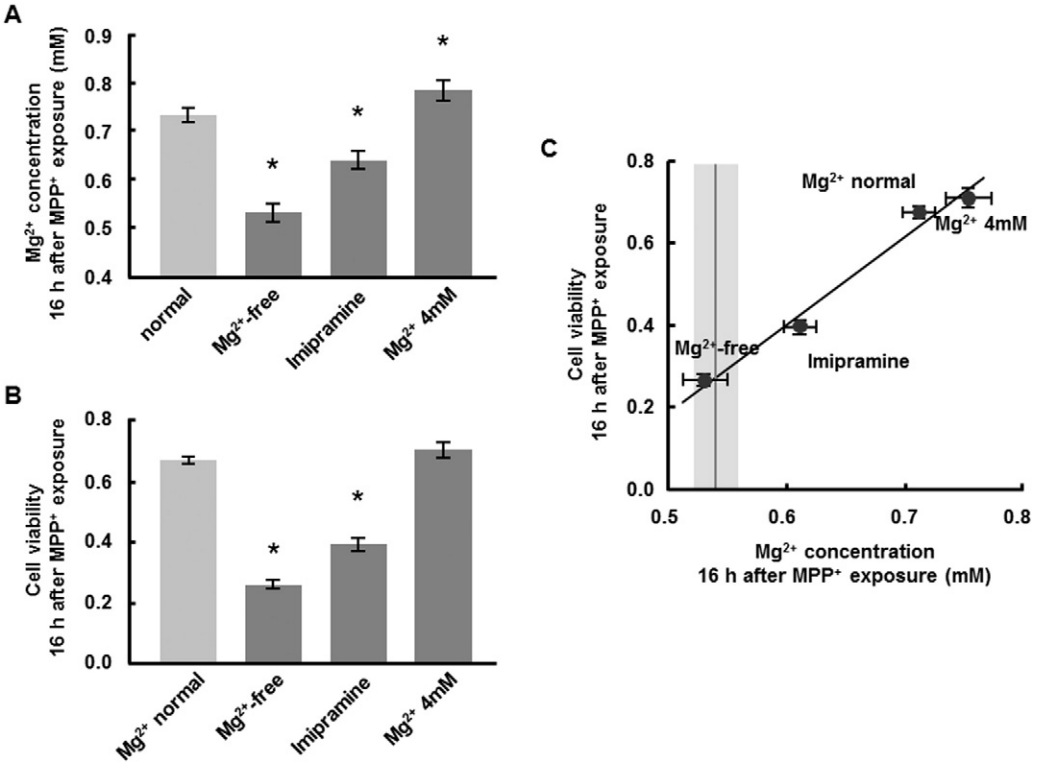

Fig. 3. Intracellular Mg^{2+} level determines cell viability. (A) Comparison of $[Mg^{2+}]_i$ after 16 h exposure to MPP^+ in normal culture medium (containing 0.8 mM Mg^{2+}, n = 563 cells from 7 experiments), in nominally Mg^{2+}-free culture medium (n = 175 cells from 4 experiments), in imipramine (40 μM) containing culture medium (n = 339 cells from 8 experiments) and in high-Mg^{2+} (4 mM) culture medium (n = 345 cells from 3 experiments). (B) Comparison of cell viability after 16 h exposure to MPP^+ in normal culture medium (n = 38), in nominally Mg^{2+}-free culture medium (n = 16), in imipramine containing culture medium (n = 16) and in high-Mg^{2+} culture medium (n = 18). (C) The cell viabilities shown in panel B were highly correlated with the $[Mg^{2+}]_i$ shown in panel A (black line, $R^2 = 0.94$). $[Mg^{2+}]_i$ in non-exposed cells (data from Fig. 2A control) was indicated as mean (gray line at 0.286 in mag-fura-2 ratio) ± SEM (light gray region). Data are represented as mean ± SEM. * indicates $P < 0.05$ in Dunnett's test.

(4 mM) conditions (Fig. 3A). The $[Mg^{2+}]_i$ in the cells exposed to MPP^+ for 16 h in each condition was correlated with the $[Mg^{2+}]_i$ concentration immediately after MPP^+ application shown in Fig. 1B. Moreover, $[Mg^{2+}]_i$ in the nominally Mg^{2+}-free medium shown in Fig. 3A was almost at the same concentration (about 0.5 mM) with that in non-treated cells (control in Fig. 2A), suggesting that the Mg^{2+} release from mitochondria had no effect on the $[Mg^{2+}]_i$ after 16 h, and the Mg^{2+} influx mainly contributed to it. Therefore, we concluded that modulation of Mg^{2+} influx alters $[Mg^{2+}]_i$ during neurodegeneration.

We examined the effect of the $[Mg^{2+}]_i$ on MPP^+-induced cell death. In a normal culture medium (DMEM containing NGF), 70% of the cells were viable after 16 h exposure to MPP^+ (Fig. 3B). In Mg^{2+}-free culture medium, the toxicity of MPP^+ accelerated, and the cell viability reduced to 25%. It also decreased to 40% in an imipramine containing culture medium. An increase in Mg^{2+} concentration in the culture medium to 4 mM partly but not significantly attenuated the toxicity. Incubation in these conditions without MPP^+ had no effect on the cell viability in 16 h (Fig. S3A). The cell viability correlated with $[Mg^{2+}]_i$ measured in the same condition ($R^2 = 0.98$, Fig. 3C). These results suggest that $[Mg^{2+}]_i$ is a crucial factor that determines cell viability in MPP^+ toxicity.

To ascertain the contribution of $[Mg^{2+}]_i$ to cell viability, $[Mg^{2+}]_i$ was altered and the effect on cell viability was estimated. When mag-fura-2-AM was used at 10 μM, MPP^+-induced increase in $[Mg^{2+}]_i$ was not observed (Fig. 4A). Since the fluorescent ion probes bind to the targeted ion, they also act as chelators of targeted ions and an excessive load of probe to cells affects cellular ion dynamics. MPP^+-induced Mg^{2+} increase was not observed by using mag-fura-2-AM at higher concentration than 5 μM (Figure S4). The cell viability after 16 h exposure to MPP^+ was significantly decreased in the Mg^{2+}-chelated cells (Fig. 4B). This concentration of mag-fura-2 had no effect on cell viability in the culture medium without MPP^+ in 16 h (Fig. S3B). Next, we tried to increase $[Mg^{2+}]_i$ and estimate the effect of high $[Mg^{2+}]_i$ on MPP^+ toxicity. To achieve it, PC12 cells stably overexpressing one of the Mg^{2+} transporters, SLC41A2, which has been reported to increase Mg^{2+} influx across the cell membrane [37], was prepared. Expression level of SLC41A2 in constitutively overexpressed cells was 1.8-fold higher than that in control cells (Fig. S5). Although it has been reported that SLC41A2 is localized to organelle's membrane [38], constitutively overexpressed SLC41A2 tagged by EGFP was localized not only to intracellular compartments but also to plasma membrane (Fig. S6). The authors pointed out the possibility that the plasma membrane localization of SLC41A2 reflect aberrant cell surface transport due to overexpression [38]; it successfully achieved to increase $[Mg^{2+}]_i$ under steady state compared with that in normal cells (control). Cell viability after a 16 h exposure to MPP^+ was also higher in overexpressed cells (Fig. 5B). These results indicate that $[Mg^{2+}]_i$ is an important factor that determines the cell viability in MPP^+ toxicity, and overexpression of SLC41A2 attenuates the toxicity by increasing $[Mg^{2+}]_i$. The next question is whether this Mg^{2+} transport protein alters the expression level in the progress of PD. We estimated the relative expression level of mRNA encoding SLC41A2 using real-time PCR at 8 and 16 h after MPP^+ treatment and compared with that of non-treated cells. It increased to 1.8 fold compared to non-treated cells after 16 h exposure to MPP^+ (Fig. 5C).

3.5. Mg^{2+} works as an inhibitor of ROS generation and maintains cellular ATP concentration

Previous studies indicate that mitochondrial dysfunction and acceleration of ROS production are typical features observed in the neurodegeneration in PD [8]. Mitochondrial activities link to cellular ATP synthesis, and ROS is one of the key regulators of MPP^+ induced cell death. $[Mg^{2+}]_i$ would attribute to these regulators of neurodegeneration before the onset of cell death. Therefore, the effect of the altered $[Mg^{2+}]_i$ was investigated to determine any effect on cellular ATP concentration and ROS generation at 8 h after MPP^+ exposure, when the viability started to decrease (Fig. S1). ATP concentration, which was measured with an ATP sensor, ATeam [28], decreased significantly in the cells exposed to MPP^+ for 8 h in a nominally Mg^{2+}-free culture medium (Fig. 6). This result indicates that Mg^{2+} is required for maintaining cellular ATP concentration. ROS generation after an 8 h exposure to MPP^+ accelerated in the cells exposed to MPP^+ in a nominally Mg^{2+}-free culture medium, and it was inhibited in the cells in a high Mg^{2+} culture medium (Fig. 7). These data indicate that effects of the increase in $[Mg^{2+}]_i$ are maintaining cellular ATP production and inhibition of ROS generation. As a consequence, the increase in $[Mg^{2+}]_i$ protects dopaminergic cells from neurodegeneration in PD.

4. Discussion

4.1. Summary of this work

Recent studies have demonstrated that Mg^{2+} is an indispensable ion for ordinal cellular functions [20,21]. Therefore, a disturbed Mg^{2+} homeostasis has been implicated in a number of diseases [39–41]. In the case of PD, it has been shown that Mg^{2+} has protective effects in vivo and in vitro experiments [26,42]. However, the underlying mechanisms remain obscure. In this study, we investigated intracellular Mg^{2+} concentration and its effect on neurodegeneration in the MPP^+ model of PD in neuronally differentiated PC12 cells. The results of our experiments showed that: 1) MPP^+ induced an increase in $[Mg^{2+}]_i$

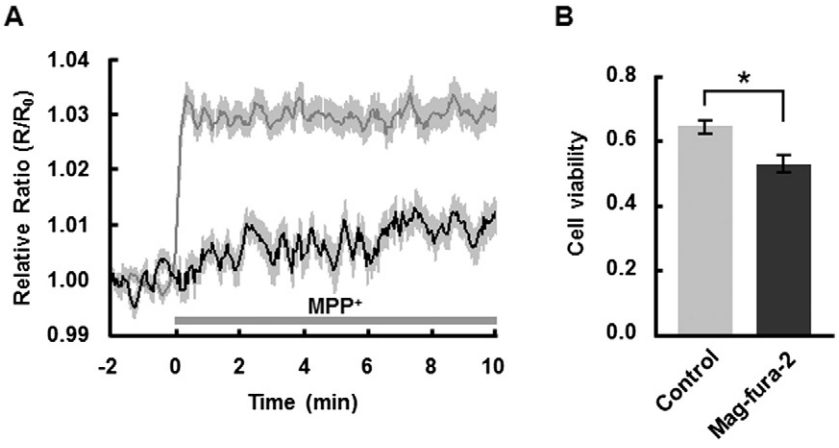

Fig. 4. Chelation of intracellular Mg^{2+} accelerated the toxicity of MPP^+. (A) Averaged time-courses of the changes in mag-fura-2 ratio in response to MPP^+ in the cells loaded with mag-fura-2-AM at 10 μM (black line, n = 67 cells from 4 experiments) and at 2 μM (gray line, n = 207 cells from 16 experiments, the same data as Fig. 1A control). (B) Comparison of cell viabilities after 16 h exposure to MPP^+ in normal culture medium (Control, n = 12) and in culture medium containing 10 μM of mag-fura-2-AM (mag-fura-2, n = 12). Data are represented as mean ± SEM. * indicates $P < 0.05$ in *t*-test.

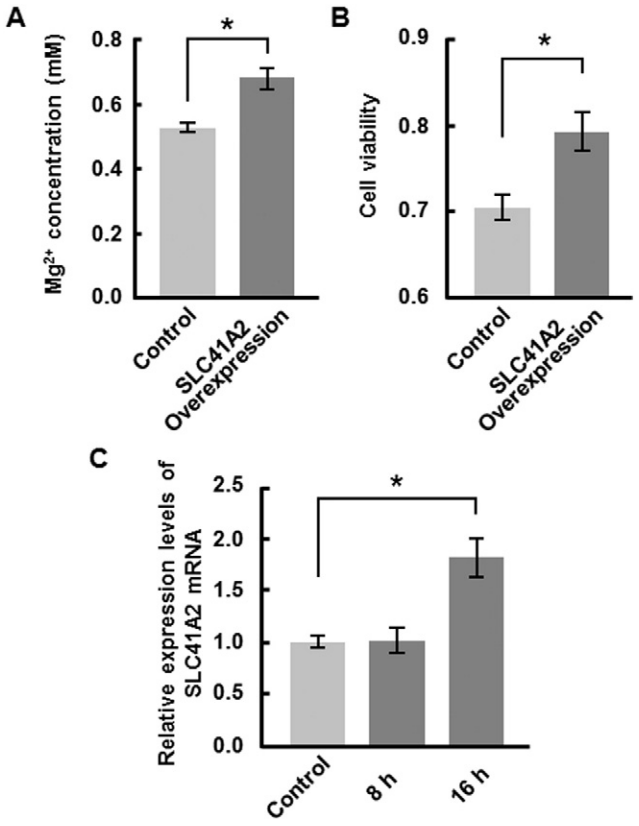

Fig. 5. Increase in $[Mg^{2+}]_i$ attenuated the toxicity of MPP^+. (A) Comparison of $[Mg^{2+}]_i$ in control cells (n = 444 cells from 9 experiments) and in SLC41A2 overexpressed cells (n = 232 cells from 9 experiments) in steady state. (B) Comparison of cell viability after 16 h exposure to MPP^+ in control cells (n = 36) and in SLC41A2 overexpressed cells (n = 36). (C) Comparison of mRNA expression levels of SLC41A2 in non-exposed cells (control) and in the cells exposed to 3 mM of MPP^+ for 8 and 16 h (n = 10 samples for each). Data are represented as mean ± SEM. * indicates $P < 0.05$ in *t*-test (A and B) and Dunnett's test (C).

immediately after its application, and it was composed of both mobilization from the mitochondria and an influx across the cell membrane (Fig. 1), 2) the Mg^{2+} influx sustained and resulted in the chronic increase in $[Mg^{2+}]_i$ and cellular total Mg^{2+} concentration (Fig. 2),

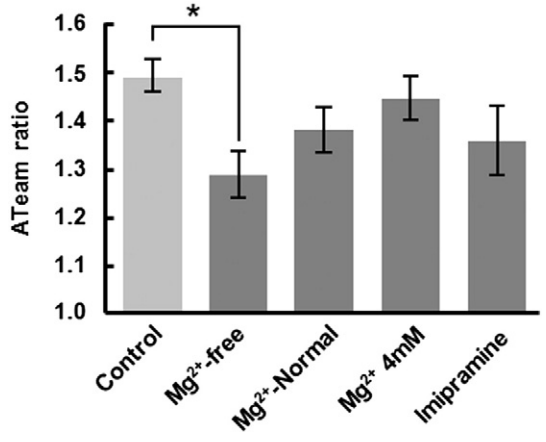

Fig. 6. Effects of $[Mg^{2+}]_i$ on cellular ATP concentration. Comparison of ATeam ratio, which corresponds to cellular ATP concentration, in non-exposed cells (Control, n = 80 cells from 4 experiments), the cells after 8 h exposure to MPP^+ in nominally Mg^{2+}-free culture medium (n = 75 cells from 4 experiments), in normal culture medium (n = 79 cells from 4 experiments), in Mg^{2+} 4 mM culture medium (n = 76 cells from 4 experiments) and Imipramine (40 μM) containing culture medium (n = 54 cells from 3 experiments). Data are represented as mean ± SEM. * indicates $P < 0.05$ in Dunnett's test.

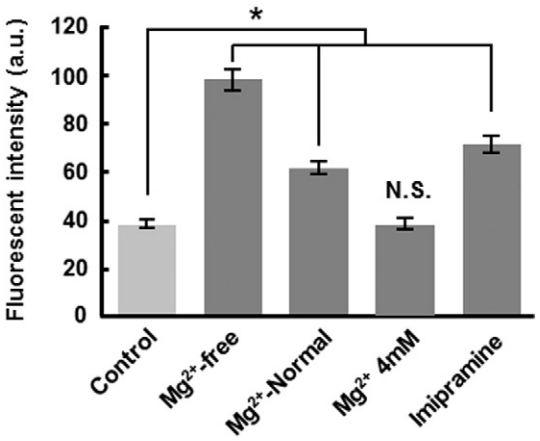

Fig. 7. Effects of $[Mg^{2+}]_i$ on cellular ROS amount. Comparison of intracellular ROS in non-exposed cells (Control, n = 540 cells from 4 experiments), in the cells after 8 h exposure to MPP^+ in nominally Mg^{2+}-free culture medium (n = 549 cells from 5 experiments), normal culture medium (n = 652 cells from 5 experiments) Mg^{2+} 4 mM culture medium (n = 740 cells from 5 experiments) and imipramine (40 μM) containing culture medium (n = 670 cells from 5 experiments). Fluorescent intensity of ROS detection probe corresponds to intracellular ROS. Data are represented as mean ± SEM. * indicates $P < 0.05$ in Dunnett's test.

3) modulation of Mg^{2+} influx altered $[Mg^{2+}]_i$ during MPP^+-induced neurodegeneration (Fig. 3), 4) the viability of the cells exposed to MPP^+ was altered depending on intracellular Mg^{2+} level (Figs. 3–5), and 5) the cellular ATP concentration was maintained and ROS generation was suppressed by the increased $[Mg^{2+}]_i$ (Fig. 6, 7). We demonstrated that MPP^+ induced an increase in $[Mg^{2+}]_i$ in neuronally differentiated PC12 cells. Whereas MPP^+ is a neurotoxic reagent, MPP^+-induced increase in $[Mg^{2+}]_i$ attenuated the toxicity. MPP^+ elicited these two effects concomitantly. It caused to elucidate a crucial role for Mg^{2+} in the neuroprotection in MPP^+ model of PD. Although a previous study revealed that supplementation of Mg^{2+} in a culture medium has a protective effect on neurodegeneration in MPP^+ model of PD [26], the underlying mechanisms have still been obscure. Our data obtained in this study clearly showed that intracellular Mg^{2+} prevents the generation of ROS, which is a main mediator of neurodegeneration in PD, and maintains cellular ATP concentration, resulting in neuroprotection. To the best of our knowledge, this is the first study that clarifies the underlying mechanisms in the protective effect of Mg^{2+} in the cellular model of PD.

4.2. Cellular Mg^{2+} transport induced by MPP^+

In this study, we demonstrated that MPP^+, which is an inducer of PD-like neurodegeneration in dopaminergic cells, elicits an increase in $[Mg^{2+}]_i$ via two different pathways (Fig. 1). The primary pathway is Mg^{2+} influx from an extracellular medium. Although what protein permeated Mg^{2+} in response to MPP^+ is still obscure, our data suggest that one possible channel is TRPM7 because 2-APB, which is an inhibitor of Mg^{2+} transport via this channel, partly attenuated an MPP^+-induced increase in $[Mg^{2+}]_i$ and mostly suppressed the $[Ca^{2+}]_i$ response (Fig. 1B and D). Moreover, imipramine, which is known as an inhibitor of Na^+/Mg^{2+} owing to Mg^{2+} extrusion and also inhibits Mg^{2+} influx via TRPM-like channel [34], attenuated the MPP^+-induced $[Mg^{2+}]_i$ influx (Fig. 1B). These inhibitors attenuated but not completely suppressed the Mg^{2+} influx at used concentrations. In imipramine treated cells, $[Mg^{2+}]_i$ and viability were significantly higher than those in the cells in a nominally Mg^{2+}-free culture medium after 16 h exposure to MPP^+ (Fig. 3) analyzed in a Tukey's test. It results from the incomplete inhibition of Mg^{2+} influx possibly via TRPM7 by 40 μM of imipramine or 50 μM of 2-APB or an existence of the other channels or transporters involved in this Mg^{2+} influx. MPP^+ chronically

activates Mg^{2+} influx, and it results in a gradual increase in $[Mg^{2+}]_i$ for 16 h (Fig. 2).

MPP^+ also induced Mg^{2+} release from mitochondria. In our previous study, we showed that MPP^+, which acts as an inhibitor of complex I in mitochondrial electron transfer chain, induces depolarization of mitochondrial membrane potential and decreases in Mg^{2+} concentration in mitochondria [25]. Rotenone, which also inhibits complex I, also induced a slight increase in $[Mg^{2+}]_i$ that probably resulted from an Mg^{2+} release from mitochondria (Fig. S7). These data suggest that MPP^+-induced Mg^{2+} release from mitochondria occurs concomitantly with the depolarization of their membrane potential induced by the inhibition of electron transfer chain. Although we had demonstrated that collapse of mitochondrial membrane potential results in Mg^{2+} release to cytoplasm [14], what protein permeates Mg^{2+} is still obscure. One possible pathway is Mg-ATP/P_i carrier, which exchanges Mg-ATP for P_i electroneutrally [43]. Since ATP-Mg/P_i carriers are activated by an increase in $[Ca^{2+}]_i$ [44], increased $[Ca^{2+}]_i$ induced by MPP^+ application might activate this protein resulting in Mg-ATP release from a mitochondrial matrix. Recently, Mg^{2+} exporter protein on mitochondrial membrane was reported in yeast mitochondria [45]. In mammalian cells, a similar protein might extrude Mg^{2+} from a mitochondrial matrix. Because mitochondrial damage is an important hallmark of human PD, an Mg^{2+} release from mitochondria possibly occurs in dopaminergic neurons in PD patients.

MPP^+ induced about 150 μM increase in $[Mg^{2+}]_i$ via two pathways described above. Mg^{2+} release from mitochondria induced by rotenone was suppressed by the use of mag-fura-2-AM at 10 μM (Fig. S7B). It indicates that an increase in $[Mg^{2+}]_i$ evoked by the inhibition of complex I (approximately 30 μM) could be chelated by mag-fura-2 when mag-fura-2-AM was used at 10 μM. Our data shown in Fig. 4 and S4 indicate that a high concentration of mag-fura-2 also suppressed the MPP^+-induced Mg^{2+} influx. It seems too high a concentration (more than 100 μM) to be chelated by mag-fura-2, even if the intracellular concentration of mag-fura-2 is higher than the used concentration of mag-fura-2-AM (10 μM). The Mg^{2+} influx induced by MPP^+ might require both MPP^+ and Mg^{2+} release from mitochondria. There might be a mechanism to amplify the Mg^{2+} signal.

Intracellular free ion concentration was regulated by influx, efflux, buffering by biological molecules and compartmentalization. Whereas $[Mg^{2+}]_i$ increased immediately after MPP^+ application, cellular total Mg^{2+} contents increased gradually for 16 h (Figs. 1 and 2). The difference in the time-course between ionized and total Mg^{2+} concentration may reflect a change in intracellular Mg^{2+} buffering molecules and mechanisms.

4.3. Protective effect of Mg^{2+} on mitochondrial functions

A decrease in cellular ATP concentration was observed in the cells exposed to MPP^+ in a nominally Mg^{2+}-free culture medium (Fig. 6). Mitochondrial ATP production is modulated by Mg^{2+} concentration in mitochondria [17,18]. The data presented in this study and our previous study show that MPP^+ induces Mg^{2+} release from mitochondria (Fig. 1 and [25]). This leads to a decrease in mitochondrial ATP production in MPP^+-treated cells. On the other hand, in the medium containing physiological range of Mg^{2+}, Mg^{2+} influx resulted in a sustained increase in $[Mg^{2+}]_i$ (Figs. 1 and 2). Since mitochondria are one of intracellular Mg^{2+} buffers, a part of increased $[Mg^{2+}]_i$ likely enters into mitochondria. It maintains Mg^{2+} concentration in mitochondria higher than that in the cells without Mg^{2+} influx treated with MPP^+ in a nominally Mg^{2+}-free culture medium. It would lead to the maintaining of cytoplasmic ATP concentration in the cells exposed to MPP^+ in other than nominally Mg^{2+}-free condition.

Cellular ROS production was suppressed by the increased $[Mg^{2+}]_i$, resulting in the attenuation of MPP^+ toxicity (Figs. 3 and 7). ROS is one of the main mediators of neurodegeneration in PD, and suppression of ROS generation attenuates neuronal cell death [8,46,47]. However, the contribution of Mg^{2+} to the regulation of cellular ROS generation is controversial. Although some studies have indicated that Mg^{2+} inhibits ROS production [19], others have reported that Mg^{2+} influx from TRPM7 accelerates ROS generation [48,49]. It was reported that the expression levels of glutathione S-transferase (GST) increased in the cells cultured in a low Mg^{2+} medium, and resulted in the suppression of cellular ROS levels [50]. Therefore, Mg^{2+} influx via TRPM7 may result in the increase in the amount of cellular ROS by suppressing ROS degradation [48]. On the other hand, Mg^{2+} inhibits mitochondrial ROS generation [19]. Impairing the activity of complex I, which is a component of mitochondrial electron transfer chain and target of MPP^+, leads to an increase in ROS generation in mitochondria and a subsequent decrease in glutathione (GSH) levels [8]. An increase in $[Mg^{2+}]_i$ induced by MPP^+ contributed to the inhibition of mitochondrial ROS generation rather than suppression of ROS degradation. This resulted in the suppression of cellular ROS generation as shown in Fig. 7.

4.4. Cellular Mg^{2+} transport and PD

Based on our results, Mg^{2+} concentration in dopaminergic neurons is crucial, and higher concentration in cellular basal Mg^{2+} concentration attenuates but not completely abolished the progress of neurodegeneration. Therefore, dysfunction of Mg^{2+} uptake into dopaminergic neurons, for example decreasing in Mg^{2+} concentration in brain tissue or down-regulation of cellular Mg^{2+} transport proteins, may accelerate the neurodegeneration in human brains. In this study, we showed that MPP^+ induces Mg^{2+} influx, although it is still obscure how MPP^+ activates Mg^{2+} transport protein on cell membrane. Whereas MPP^+ as well as rotenone inhibits complex I of mitochondrial electron transfer chain and elicited Mg^{2+} release from mitochondria, only MPP^+ induced Mg^{2+} influx (Fig. 1 and S7). It suggests that Mg^{2+} influx might not be elicited depending on causes of PD, because it was not observed in rotenone model of PD (Fig. S7). This may be a cause of the conflict in previous reports: there are no significant difference in Mg^{2+} concentration between tissues in PD patients and those in control [51,52], whereas other studies showed that Mg^{2+} concentration in tissues in PD patients were lowered [23,53]. Since mitochondrial damage is a critical event in human PD, Mg^{2+} release from mitochondria probably occurs in patient's brains. Cytoplasmic excess Mg^{2+} is extruded via Na^+/Mg^{2+} exchangers [54], hence it results in the decrease in cellular Mg^{2+} concentration. It may lead to the lowered Mg^{2+} concentration in the brain tissue reported [23,53]. Based on our data, it accelerates neurodegeneration. Whereas symptoms of PD develop in the neurons containing any concentration of Mg^{2+}, it is ready to occur and progress in the neurons containing low concentration of Mg^{2+}.

In this study, we observed that imipramine inhibited MPP^+-induced Mg^{2+} influx, whereas it is usually used to inhibit Na^+/Mg^{2+} exchangers for Mg^{2+} extrusion. It probably inhibited Mg^{2+} efflux via the exchangers as well as MPP^+-induced Mg^{2+} influx. Although the inhibition of Mg^{2+} efflux seems to result in an increase in $[Mg^{2+}]_i$ by accumulating mobilized Mg^{2+}, our data indicate that imipramine inhibits MPP^+-induced increase in $[Mg^{2+}]_i$. It suggests that $[Mg^{2+}]_i$ is dominantly determined by Mg^{2+} influx upon the neurodegeneration in PD.

$[Mg^{2+}]_i$ is strictly regulated by many types of Mg^{2+} specific channels and transporters on the cell membrane and on organelles [16,55]. Among those channels and transporters, mutation in TRPM7 has been reported in some familial PD patients [56,57]. It indicates that dysfunction of cellular Mg^{2+} transport is one of the risk factors of PD, since this channel plays an important role in cellular Mg^{2+} homeostasis [58,59]. This is consistent with the report that Mg^{2+} deficiency induces degeneration of dopaminergic neurons in substantia nigra in rat [42]. In our experiments, Mg^{2+} influx, which might be carried by TRPM7 (Fig. 1B), has a protective effect (Fig. 3). It suggests that this channel plays important roles not only in cellular Mg^{2+} transport but also in neuroprotection in PD patients. Because it has been shown that down-regulation

of TRPM7 could be rescued by up-regulation of other Mg^{2+} transporters such as SLC41A2 [37], the mutation in TRPM7 does not always lead to PD [60]. In our experiment, overexpression of SLC41A2 resulted in an attenuation of MPP^+ toxicity (Fig. 5B). It suggests that an increase in $[Mg^{2+}]_i$, wherever mobilized, attenuates the neurodegeneration in PD. Moreover, expression levels of mRNA encoding SLC41A2 increased in the progress of PD (Fig. 5C). It might be a cell protection mechanism against neurodegeneration by increasing $[Mg^{2+}]_i$.

It is likely that Mg^{2+} channels and transporters also work compensatorily with each other to maintain $[Mg^{2+}]_i$ in vivo. Therefore, variations of expression levels of those proteins and robustness of Mg^{2+} transport in neurons might decide a risk of neurodegenerative disorder in human brain. The progression of PD might also perturb the expression levels of those proteins, contrarily. Based on these ideas, it seems to be important to investigate changes in the expression levels of Mg^{2+} transport proteins during neurodegeneration and clarify which protein is sensitive to the progress of neurodegeneration in PD.

Author contribution statements

Y.S. designed the study, performed the experiments, analyzed the data, and wrote the manuscript; R.Y. analyzed the data; K.S., K.H. and K.O. designed and supervised the study. All authors reviewed the manuscript.

Competing financial interests

The authors declare no competing financial interests.

Transparency document

The Transparency document associated with this article can be found, in the version.

Acknowledgments

We thank Dr. H. Imamura and Dr. H. Noji for providing the ATeam plasmid. We also thank Mr. Shibata in Shimadzu Science and Mr. Seki in Asahi Lifescience for providing the osmometer. This research was supported by a Grant-in-Aid for Scientific Research, KAKENHI (24240045 and 25750395), and Strategic Research Foundation Grant-aided Project for Private Universities from the Ministry of Education, Culture, Sport, Science, and Technology, Japan (MEXT), (2014–2018, S1411003).

Appendix A. Supplementary data

Supplementary data to this article can be found online at http://dx.doi.org/10.1016/j.bbamcr.2015.08.013.

References

[1] R.B. Mounsey, P. Teismann, Mitochondrial dysfunction in Parkinson's disease: pathogenesis and neuroprotection, Park. Dis. 2011 (2011) 617472.
[2] A.H. Schapira, Mitochondrial disease, Lancet 368 (2006) 70–82.
[3] P.M. Abou-Sleiman, M.M. Muqit, N.W. Wood, Expanding insights of mitochondrial dysfunction in Parkinson's disease, Nat. Rev. Neurosci. 7 (2006) 207–219.
[4] P.A. Trimmer, R.H. Swerdlow, J.K. Parks, P. Keeney, J.P. Bennett Jr., S.W. Miller, R.E. Davis, W.D. Parker Jr., Abnormal mitochondrial morphology in sporadic Parkinson's and Alzheimer's disease cybrid cell lines, Exp. Neurol. 162 (2000) 37–50.
[5] X. Wang, T.G. Petrie, Y. Liu, J. Liu, H. Fujioka, X. Zhu, Parkinson's disease-associated DJ-1 mutations impair mitochondrial dynamics and cause mitochondrial dysfunction, J. Neurochem. 121 (2012) 830–839.
[6] G.L. McLelland, V. Soubannier, C.X. Chen, H.M. McBride, E.A. Fon, Parkin and PINK1 function in a vesicular trafficking pathway regulating mitochondrial quality control, EMBO J. 33 (2014) 282–295.
[7] P. Seibler, J. Graziotto, H. Jeong, F. Simunovic, C. Klein, D. Krainc, Mitochondrial Parkin recruitment is impaired in neurons derived from mutant PINK1 induced pluripotent stem cells, J. Neurosci. 31 (2011) 5970–5976.
[8] V. Dias, E. Junn, M.M. Mouradian, The role of oxidative stress in Parkinson's disease, J. Park. Dis. 3 (2013) 461–491.
[9] A.K. Liou, Z. Zhou, W. Pei, T.M. Lim, X.M. Yin, J. Chen, BimEL up-regulation potentiates AIF translocation and cell death in response to MPTP, FASEB J. 19 (2005) 1350–1352.
[10] H. Kang, B.S. Han, S.J. Kim, Y.J. Oh, Mechanisms to prevent caspase activation in rotenone-induced dopaminergic neurodegeneration: role of ATP depletion and procaspase-9 degradation, Apoptosis 17 (2012) 449–462.
[11] T. Fujii, Y. Shindo, K. Hotta, D. Citterio, S. Nishiyama, K. Suzuki, K. Oka, Design and synthesis of a FlAsH-type Mg^{2+} fluorescent probe for specific protein labeling, J. Am. Chem. Soc. 136 (2014) 2374–2381.
[12] R. Yamanaka, Y. Shindo, K. Hotta, K. Suzuki, K. Oka, NO/cGMP/PKG signaling pathway induces magnesium release mediated by mitoK channel opening in rat hippocampal neurons, FEBS Lett. 587 (2013) 2643–2648.
[13] Y. Shindo, A. Fujimoto, K. Hotta, K. Suzuki, K. Oka, Glutamate-induced calcium increase mediates magnesium release from mitochondria in rat hippocampal neurons, J. Neurosci. Res. 88 (2010) 3125–3132.
[14] T. Kubota, Y. Shindo, K. Tokuno, H. Komatsu, H. Ogawa, S. Kudo, Y. Kitamura, K. Suzuki, K. Oka, Mitochondria are intracellular magnesium stores: investigation by simultaneous fluorescent imagings in PC12 cells, Biochim. Biophys. Acta 1744 (2005) 19–28.
[15] F.I. Wolf, V. Trapani, Cell (patho)physiology of magnesium, Clin. Sci. (Lond.) 114 (2008) 27–35.
[16] A.M. Romani, Cellular magnesium homeostasis, Arch. Biochem. Biophys. 512 (2011) 1–23.
[17] A. Panov, A. Scarpa, Mg^{2+} control of respiration in isolated rat liver mitochondria, Biochemistry 35 (1996) 12849–12856.
[18] J.S. Rodriguez-Zavala, R. Moreno-Sanchez, Modulation of oxidative phosphorylation by Mg^{2+} in rat heart mitochondria, J. Biol. Chem. 273 (1998) 7850–7855.
[19] A.J. Kowaltowski, E.S. Naia-da-Silva, R.F. Castilho, A.E. Vercesi, Ca^{2+}-stimulated mitochondrial reactive oxygen species generation and permeability transition are inhibited by dibucaine or Mg^{2+}, Arch. Biochem. Biophys. 359 (1998) 77–81.
[20] F.Y. Li, B. Chaigne-Delalande, C. Kanellopoulou, J.C. Davis, H.F. Matthews, D.C. Douek, J.I. Cohen, G. Uzel, H.C. Su, M.J. Lenardo, Second messenger role for Mg^{2+} revealed by human T-cell immunodeficiency, Nature 475 (2011) 471–476.
[21] J. Jin, L.J. Wu, J. Jun, X. Cheng, H. Xu, N.C. Andrews, D.E. Clapham, The channel kinase, TRPM7, is required for early embryonic development, Proc. Natl. Acad. Sci. U. S. A. 109 (2012) E225–E233.
[22] N. Palacios-Prado, S. Chapuis, A. Panjkovich, J. Fregeac, J.I. Nagy, F.F. Bukauskas, Molecular determinants of magnesium-dependent synaptic plasticity at electrical synapses formed by connexin36, Nat. Commun. 5 (2014) 4667.
[23] M. Yasui, T. Kihira, K. Ota, Calcium, magnesium and aluminum concentrations in Parkinson's disease, Neurotoxicology 13 (1992) 593–600.
[24] M. Kolisek, G. Sponder, L. Mastrototaro, A. Smorodchenko, P. Launay, J. Vormann, M. Schweigel-Rontgen, Substitution p.A350V in Na(+)/Mg(2+) exchanger SLC41A1, potentially associated with Parkinson's disease, is a gain-of-function mutation, PLoS One 8 (2013), e71096.
[25] Y. Shindo, T. Fujii, H. Komatsu, D. Citterio, K. Hotta, K. Suzuki, K. Oka, Newly developed Mg^{2+}-selective fluorescent probe enables visualization of Mg^{2+} dynamics in mitochondria, PLoS One 6 (2011), e23684.
[26] T. Hashimoto, K. Nishi, J. Nagasao, S. Tsuji, K. Oyanagi, Magnesium exerts both preventive and ameliorating effects in an in vitro rat Parkinson disease model involving 1-methyl-4-phenylpyridinium (MPP^+) toxicity in dopaminergic neurons, Brain Res. 1197 (2008) 143–151.
[27] G. Grynkiewicz, M. Poenie, R.Y. Tsien, A new generation of Ca^{2+} indicators with greatly improved fluorescence properties, J. Biol. Chem. 260 (1985) 3440–3450.
[28] H. Imamura, K.P. Nhat, H. Togawa, K. Saito, R. Iino, Y. Kato-Yamada, T. Nagai, H. Noji, Visualization of ATP levels inside single living cells with fluorescence resonance energy transfer-based genetically encoded indicators, Proc. Natl. Acad. Sci. U. S. A. 106 (2009) 15651–15656.
[29] A.K. Stout, I.J. Reynolds, High-affinity calcium indicators underestimate increases in intracellular calcium concentrations associated with excitotoxic glutamate stimulations, Neuroscience 89 (1999) 91–100.
[30] V. Trapani, G. Farruggia, C. Marraccini, S. Iotti, A. Cittadini, F.I. Wolf, Intracellular magnesium detection: imaging a brighter future, Analyst 135 (2010) 1855–1866.
[31] L.V. Ryazanova, L.J. Rondon, S. Zierler, Z. Hu, J. Galli, T.P. Yamaguchi, A. Mazur, A. Fleig, A.G. Ryazanov, TRPM7 is essential for Mg(2+) homeostasis in mammals, Nat. Commun. 1 (2010) 109.
[32] M.D. Bootman, T.J. Collins, L. Mackenzie, H.L. Roderick, M.J. Berridge, C.M. Peppiatt, 2-Aminoethoxydiphenyl borate (2-APB) is a reliable blocker of store-operated Ca^{2+} entry but an inconsistent inhibitor of InsP3-induced Ca^{2+} release, FASEB J. 16 (2002) 1145–1150.
[33] T. Hanano, Y. Hara, J. Shi, H. Morita, C. Umebayashi, E. Mori, H. Sumimoto, Y. Ito, Y. Mori, R. Inoue, Involvement of TRPM7 in cell growth as a spontaneously activated Ca^{2+} entry pathway in human retinoblastoma cells, J. Pharmacol. Sci. 95 (2004) 403–419 (Epub 2004 Jul 2024).
[34] Y. Hamaguchi, Y. Tatematsu, K. Furukawa, T. Matsubara, S. Nakayama, Imipramine inhibition of TRPM-like plasmalemmal Mg^{2+} transport in vascular smooth muscle cells, J. Cell. Mol. Med. 15 (2011) 593–601.
[35] C. Cefaratti, A. Romani, A. Scarpa, Differential localization and operation of distinct Mg(2+) transporters in apical and basolateral sides of rat liver plasma membrane, J. Biol. Chem. 275 (2000) 3772–3780.
[36] B. Zhivotovsky, S. Orrenius, Calcium and cell death mechanisms: a perspective from the cell death community, Cell Calcium 50 (2011) 211–221.
[37] J. Sahni, B. Nelson, A.M. Scharenberg, SLC41A2 encodes a plasma-membrane Mg^{2+} transporter, Biochem. J. 401 (2007) 505–513.

[38] J. Sahni, A.M. Scharenberg, The SLC41 family of MgtE-like magnesium transporters, Mol. Aspects Med. 34 (2013) 620–628.
[39] A. Yogi, G.E. Callera, T.T. Antunes, R.C. Tostes, R.M. Touyz, Transient receptor potential melastatin 7 (TRPM7) cation channels, magnesium and the vascular system in hypertension, Circ. J. 75 (2011) 237–245.
[40] M.D. Boska, K.M. Welch, P.B. Barker, J.A. Nelson, L. Schultz, Contrasts in cortical magnesium, phospholipid and energy metabolism between migraine syndromes, Neurology 58 (2002) 1227–1233.
[41] M. Barbagallo, L.J. Dominguez, Magnesium metabolism in type 2 diabetes mellitus, metabolic syndrome and insulin resistance, Arch. Biochem. Biophys. 458 (2007) 40–47.
[42] K. Oyanagi, E. Kawakami, K. Kikuchi-Horie, K. Ohara, K. Ogata, S. Takahama, M. Wada, T. Kihira, M. Yasui, Magnesium deficiency over generations in rats with special references to the pathogenesis of the Parkinsonism-dementia complex and amyotrophic lateral sclerosis of Guam, Neuropathology 26 (2006) 115–128.
[43] J. Satrustegui, B. Pardo, A. Del Arco, Mitochondrial transporters as novel targets for intracellular calcium signaling, Physiol. Rev. 87 (2007) 29–67.
[44] M.T. Nosek, D.T. Dransfield, J.R. Aprille, Calcium stimulates ATP-Mg/Pi carrier activity in rat liver mitochondria, J. Biol. Chem. 265 (1990) 8444–8450.
[45] Y. Cui, S. Zhao, J. Wang, X. Wang, B. Gao, Q. Fan, F. Sun, B. Zhou, A novel mitochondrial carrier protein Mme1 acts as a yeast mitochondrial magnesium exporter, Biochim. Biophys. Acta 1854 (2015) 724–732.
[46] F. Yi, X. He, D. Wang, Lycopene protects against MPP(+)-induced cytotoxicity by maintaining mitochondrial function in SH-SY5Y cells, Neurochem. Res. 38 (2013) 1747–1757.
[47] J. Chen, X.Q. Tang, J.L. Zhi, Y. Cui, H.M. Yu, E.H. Tang, S.N. Sun, J.Q. Feng, P.X. Chen, Curcumin protects PC12 cells against 1-methyl-4-phenylpyridinium ion-induced apoptosis by bcl-2–mitochondria–ROS–iNOS pathway, Apoptosis 11 (2006) 943–953.
[48] H.C. Chen, L.T. Su, O. Gonzalez-Pagan, J.D. Overton, L.W. Runnels, A key role for Mg(2+) in TRPM7's control of ROS levels during cell stress, Biochem. J. 445 (2012) 441–448.
[49] A. Yogi, G.E. Callera, S. O'Connor, T.T. Antunes, W. Valinsky, P. Miquel, A.C. Montezano, A.L. Perraud, C. Schmitz, A. Shrier, R.M. Touyz, Aldosterone signaling through transient receptor potential melastatin 7 cation channel (TRPM7) and its alpha-kinase domain, Cell. Signal. 25 (2013) 2163–2175.
[50] F.I. Wolf, V. Trapani, M. Simonacci, A. Boninsegna, A. Mazur, J.A. Maier, Magnesium deficiency affects mammary epithelial cell proliferation: involvement of oxidative stress, Nutr. Cancer 61 (2009) 131–136.
[51] B. Bocca, A. Alimonti, O. Senofonte, A. Pino, N. Violante, F. Petrucci, G. Sancesario, G. Forte, Metal changes in CSF and peripheral compartments of parkinsonian patients, J. Neurol. Sci. 248 (2006) 23–30.
[52] I. Hozumi, T. Hasegawa, A. Honda, K. Ozawa, Y. Hayashi, K. Hashimoto, M. Yamada, A. Koumura, T. Sakurai, A. Kimura, Y. Tanaka, M. Satoh, T. Inuzuka, Patterns of levels of biological metals in CSF differ among neurodegenerative diseases, J. Neurol. Sci. 303 (2011) 95–99.
[53] G. Forte, A. Alimonti, N. Violante, M. Di Gregorio, O. Senofonte, F. Petrucci, G. Sancesario, B. Bocca, Calcium, copper, iron, magnesium, silicon and zinc content of hair in Parkinson's disease, J. Trace Elem. Med. Biol. 19 (2005) 195–201.
[54] T. Kubota, K. Tokuno, J. Nakagawa, Y. Kitamura, H. Ogawa, Y. Suzuki, K. Suzuki, K. Oka, Na^{+}/Mg^{2+} transporter acts as a Mg^{2+} buffering mechanism in PC12 cells, Biochem. Biophys. Res. Commun. 303 (2003) 332–336.
[55] G.A. Quamme, Molecular identification of ancient and modern mammalian magnesium transporters, Am. J. Physiol. Cell Physiol. 298 (2010) C407–C429.
[56] M.C. Hermosura, R.M. Garruto, TRPM7 and TRPM2—candidate susceptibility genes for Western Pacific ALS and PD? Biochim. Biophys. Acta 1772 (2007) 822–835.
[57] M.C. Hermosura, H. Nayakanti, M.V. Dorovkov, F.R. Calderon, A.G. Ryazanov, D.S. Haymer, R.M. Garruto, A TRPM7 variant shows altered sensitivity to magnesium that may contribute to the pathogenesis of two Guamanian neurodegenerative disorders, Proc. Natl. Acad. Sci. U. S. A. 102 (2005) 11510–11515.
[58] M.J. Nadler, M.C. Hermosura, K. Inabe, A.L. Perraud, Q. Zhu, A.J. Stokes, T. Kurosaki, J.P. Kinet, R. Penner, A.M. Scharenberg, A. Fleig, LTRPC7 is a Mg.ATP-regulated divalent cation channel required for cell viability, Nature 411 (2001) 590–595.
[59] C. Schmitz, A.L. Perraud, C.O. Johnson, K. Inabe, M.K. Smith, R. Penner, T. Kurosaki, A. Fleig, A.M. Scharenberg, Regulation of vertebrate cellular Mg^{2+} homeostasis by TRPM7, Cell 114 (2003) 191–200.
[60] K. Hara, Y. Kokubo, H. Ishiura, Y. Fukuda, A. Miyashita, R. Kuwano, R. Sasaki, J. Goto, M. Nishizawa, S. Kuzuhara, S. Tsuji, TRPM7 is not associated with amyotrophic lateral sclerosis–parkinsonism dementia complex in the Kii peninsula of Japan, Am. J. Med. Genet. B Neuropsychiatr. Genet. 153B (2010) 310–313.